Supplementary information: Model systems for dye-sensitized solar cells: cyanidin-silver nanocluster hybrids at TiO_2 support

Margarita Bužančić Milosavljević[1], Antonija Mravak[1], Martina Perić Bakulić[1,*], and Vlasta Bonačić-Koutecký[1,2,3,*]

[1]Center of Excellence for Science and Technology-Integration of Mediterranean region (STIM), Faculty of Science, University of Split, Ruđera Boškovića 33, 21000 Split, Croatia.
[2]Interdisciplinary Center for Advanced Science and Technology (ICAST) at University of Split, Meštrovićevo šetalište 45, 21000 Split, Croatia
[3]Department of Chemistry, Humboldt Universität zu Berlin, Brook-Taylor-Strasse 2, 12489 Berlin, Germany.

Photovoltaic parameters

Incident photon to conversion efficiency (IPCE) of dye-sensitized solar cells (DSSC):

$$IPCE = LHE \cdot \Phi_{injc} \cdot \eta_c \tag{1}$$

can be evaluated as a product of light harvesting efficiency (LHE), electron injection efficiency (Φ_{injc}) and charge collection efficiency (η_c).
Light harvesting efficiency is approximated using the equation:

$$LHE = 1 - 10^{-f} \tag{2}$$

where f is the oscillator strength of maximum absorption. High performance of DSSCs is related to the large value of the LHE.
Electron injection efficiency (Φ_{injc}), is proportional to the driving force (ΔG^{inject}), which corresponds to the difference between oxidation potential energy of the excited state (E_{ox}^{dye*}), and reduction potential energy of conduction band (ECB).[1]

$$E_{ox}^{dye*} = E_{ox}^{dye} - \lambda_{max} \tag{3}$$

where redox E_{ox}^{dye} is potential of the ground state, and λ_{max} is maximum absorption energy of the sensitizer. Finally, ΔG^{inject} can be written as:

$$\Delta G^{inject} = (E_{ox}^{dye} - \lambda_{max}) - ECB \tag{4}$$

$$E_{ox}^{dye} = -HOMO \tag{5}$$

Experimental ECB of TiO_2 has a value of -4 eV[2–4] vs. vacuum.
To obtain effective photo-induced electron transfer from the dye sensitizer to the semiconductor, energy levels of the highest occupied (HOMO) and lowest unoccupied (LUMO) molecular orbitals of the dye are required to match the redox potential of the electrolyte, I^-/I_3^- (-4.6 eV[5] vs. vacuum) and the conduction band edge of the semiconductor.[1]

Binding energy

The binding energy of the hybrid system E_b corresponds to the:

$$E_b = E_{hybrid} - (E_{cyanidin} + E_{NC}) \tag{6}$$

where E_{hybrid}, $E_{cyanidin}$ and E_{NC} are energies of optimized cyanidin-NC hybrid, cyanidin dye, and NC systems, respectively.

The binding (adsorption) energy E_{ads} of the cyanidin-Ag_9 at TiO_2 surface model is defined as:

$$E_{ads} = E_{complex} - (E_{TiO_2} + E_{cyanidin-Ag_9}) \tag{7}$$

$E_{complex}$ is the energy of adsorbed cyanidin-Ag_9, E_{TiO_2} is the energy of the optimized TiO_2 model and $E_{cyanidin-Ag_9}$ energy of the optimized cyanidin-Ag_9.

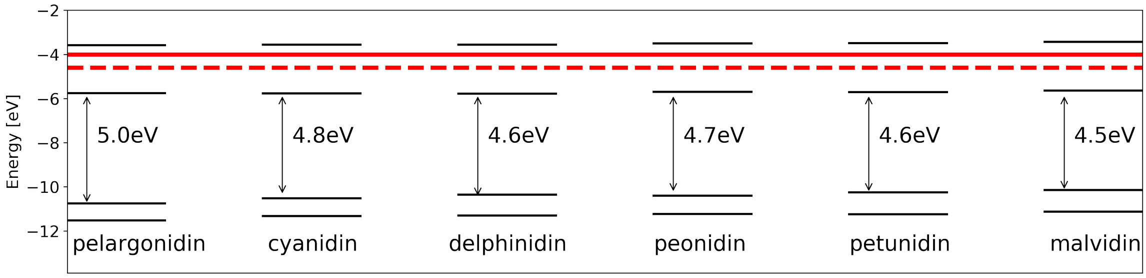

Figure S1: DFT calculated HOMO–LUMO (and HOMO-1, LUMO+1) energy gaps versus vacuum[eV] for the anthocyanidin dyes in comparison with the experimental TiO_2 conduction band edge (red line) and I^-/I_3^- redox level (dashed red line).

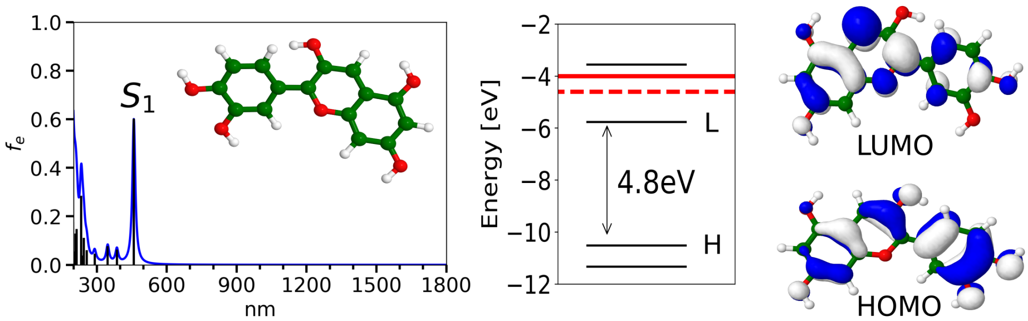

Figure S2: TDDFT calculated absorption spectrum for cyanidin dye employing CAM-B3LYP/def2-SVP method. The structure has been optimized at PBE/def2-SVP level of theory.
DFT HOMO, LUMO orbitals, and HOMO, LUMO, HOMO-1 and LUMO+1 energy gaps versus vacuum. Experimental TiO_2 conduction band edge (full red line) and I^-/I_3^- redox level (dashed red line).

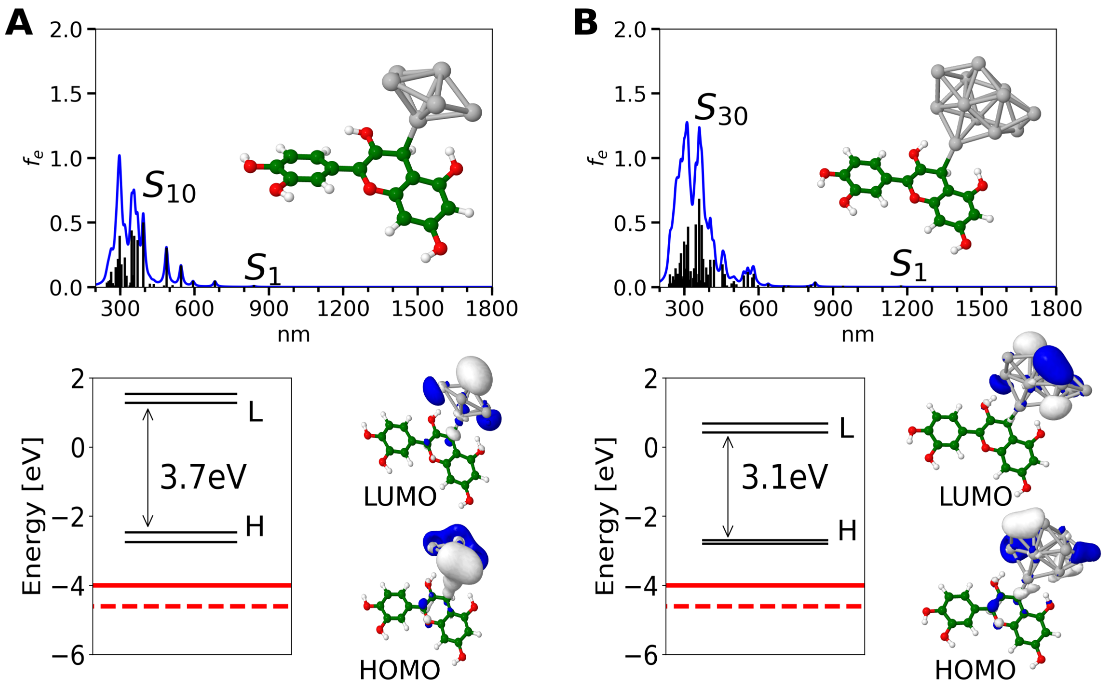

Figure S3: TDDFT calculated absorption spectra for the: A) (cyanidin-Ag_6)$^-$, B) (cyanidin-Ag_{12})$^-$ employing CAM-B3LYP/def2-SVP method. Structures have been optimized at PBE/def2-SVP level of theory.
DFT HOMO, LUMO, HOMO-1, and LUMO+1 energy gaps versus vacuum[eV] and HOMO-LUMO orbitals. Experimental TiO_2 conduction band edge (full red line) and I^-/I_3^- redox level (dashed red line)

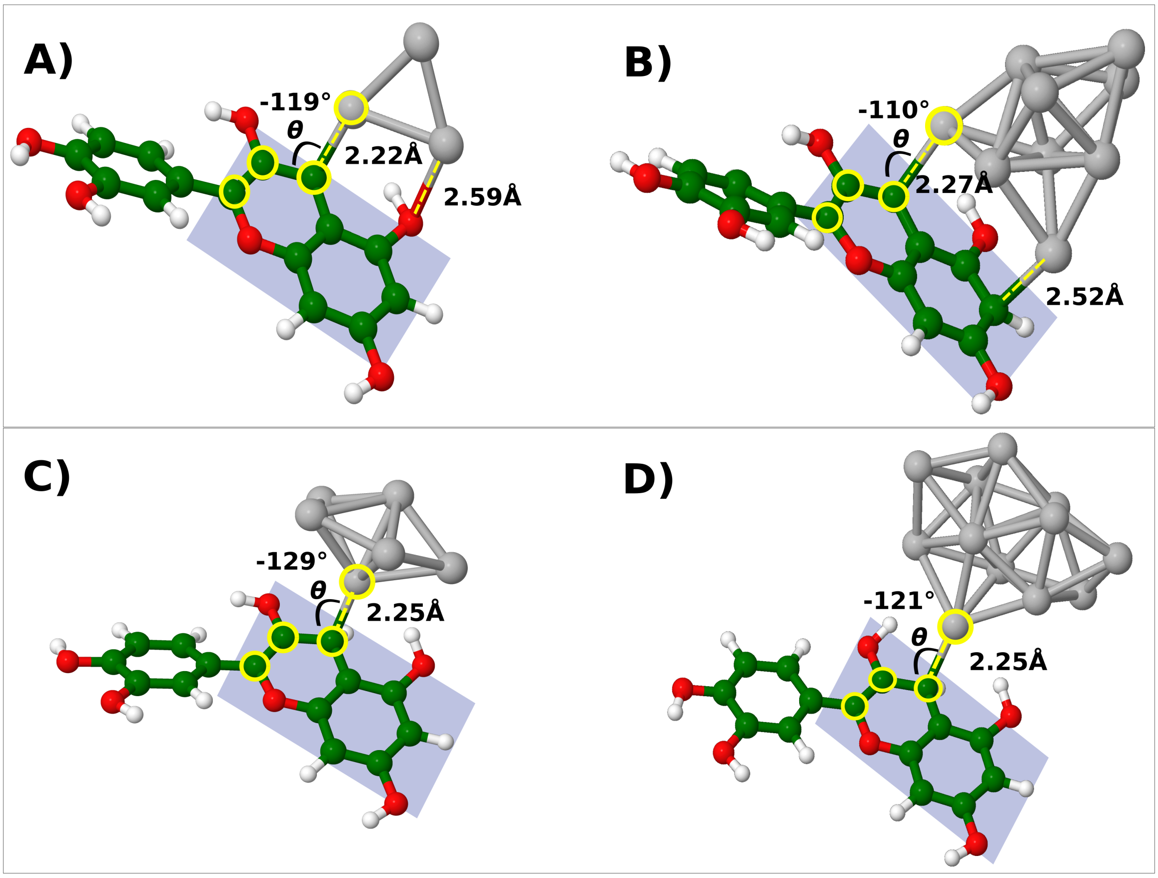

Figure S4: The bond lengths and dihedral angles between cyanidin and silver NC of hybrid systems are shown for A) cyanidin-Ag_3, B) cyanidin-Ag_9 with an even number of electrons, and C) (cyanidin-$Ag_6)^-$, D) (cyanidin-$Ag_{12})^-$ with an odd number of electrons. The blue rectangle represents the plane of the indoline group of the cyanidin dye, θ is the dihedral angle between the plane and silver NC.

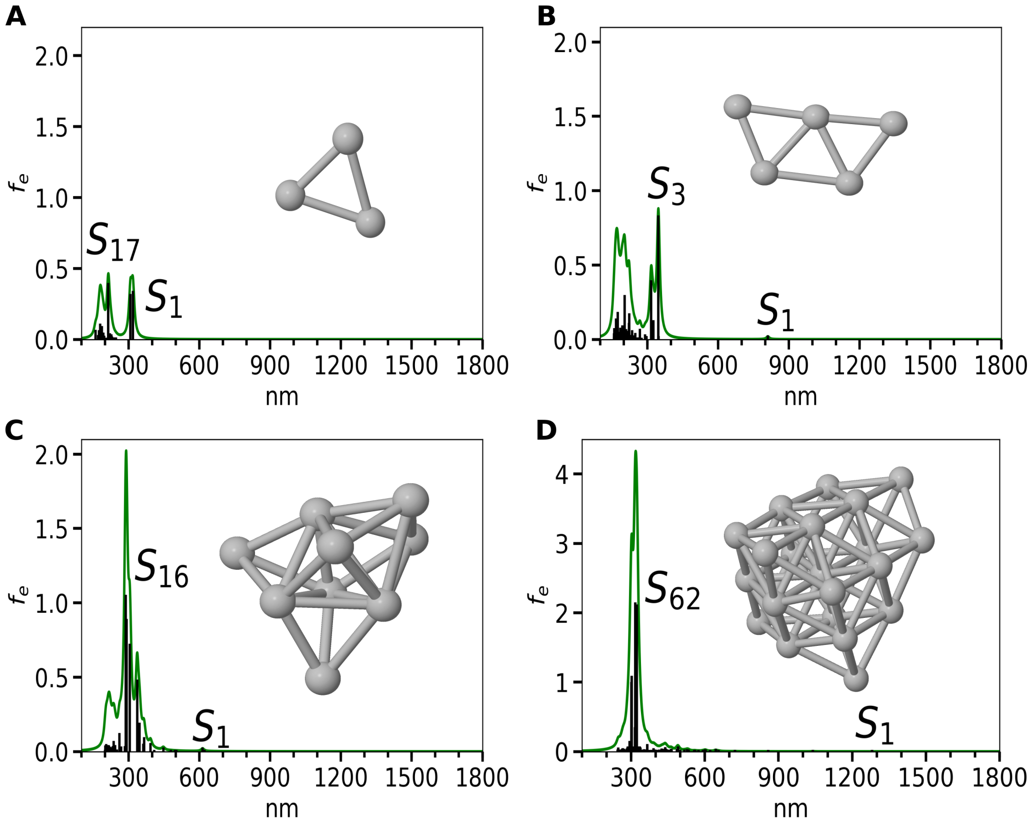

Figure S5: TDDFT calculated absorption spectra for the: A) $Ag_3{}^+$, B) $Ag_5{}^+$, C) $Ag_9{}^+$ and D) $Ag_{21}{}^+$ clusters with structures from cyanidin-NC hybrids at CAM-B3LYP/def2-SVP level of theory.

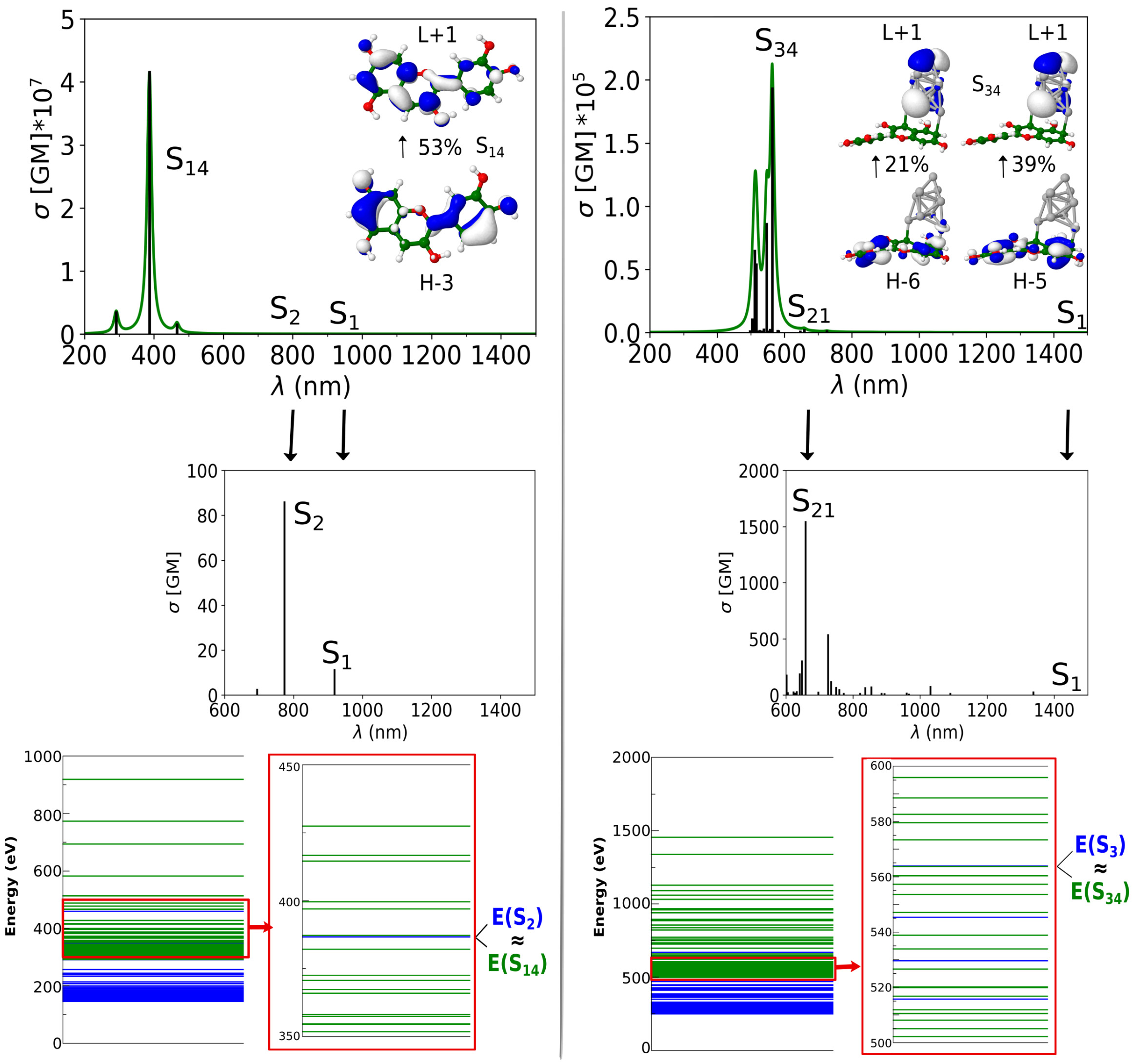

Figure S6: TPA spectra obtained by TDDFT for cyanidin (left) and cyanidin-Ag_9 (right). MO analysis is shown. TPA cross sections for states in NIR regime are also presented (middle). The resonance between OPA (blue) and TPA (green) states is included (bottom).

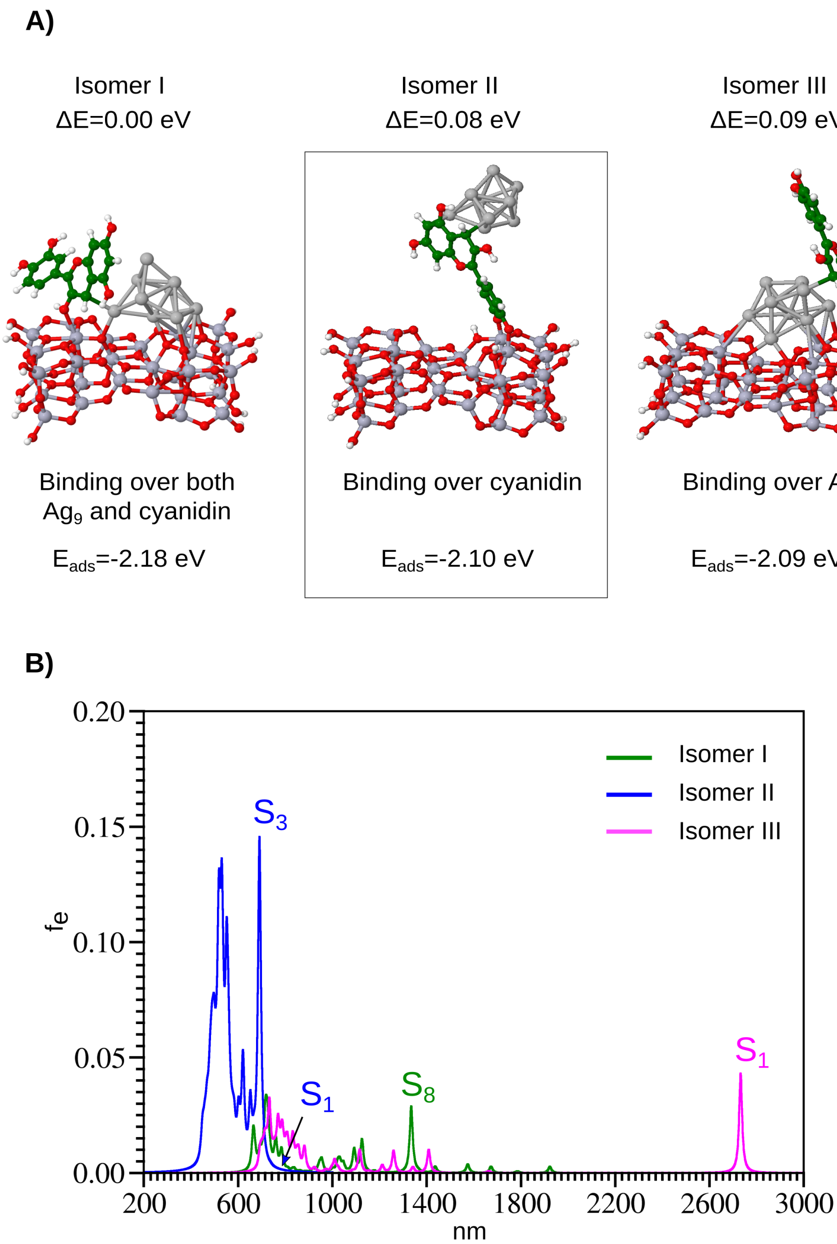

Figure S7: A) Isomers of {cyanidin-Ag_9}-TiO_2 with different adsorption modes. B) TDDFT calculated absorption spectra for isomers I, II and III of {cyanidin-Ag_9}-TiO_2 at CAM-B3LYP/def2-SVP level of theory. S_1 state of isomer I is located at 6090 nm (f_e=0.027).

Table S1: Excited states corresponding to the largest calculated absorptions for {cyanidin-Ag_9}-TiO_2 at CAM-B3LYP/def2-SVP level of theory with calculated wavelengths λ, oscillator strengths f_e and predominant transitions

Excited state	$\lambda[nm]$	f_e	Transitions
S_3	691	0.1425	H → L+25 (39%)
			H → L+26 (26%)
			H → L+29 (11%)
S_7	620	0.0440	H → L+2 (38%)
			H → L+14 (13%)
			H → L+12 (12%)
S_{14}	551	0.0742	H → L+49 (20%)
			H → L+51 (16%)
			H → L+52 (10%)
S_{18}	531	0.0868	H → L+19 (19%)
			H-1 → L+25 (15%)

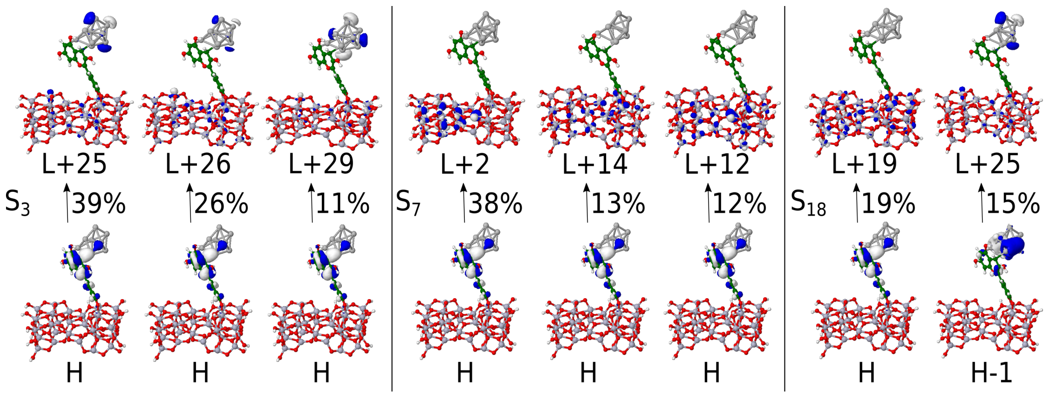

Figure S8: Transitions representing S_3, S_7 and S_{18} states are shown. S_3 state corresponds to transitions from HOMO orbital delocalized on the hybrid to higher LUMO orbitals delocalized partly at support and partly at Ag_9. The transitions associated with the excited states higher in energy (S_7, S_{18}) demonstrate clear charge transfer from HOMO (HOMO-1) to higher LUMO orbitals delocalized entirely at TiO_2 model.

References

[1] W. Fan, D. Tan, W.-Q. Deng, Acene-modified triphenylamine dyes for dye-sensitized solar cells: A computational study, ChemPhysChem 13 (8) (2012) 2051–2060. doi:https://doi.org/10.1002/cphc.201200064.

[2] M. Grätzel, Photoelectrochemical cells, Nature 414 (2001) 338–344. doi:10.1038/35104607.

[3] H.-S. Kim, C.-R. Lee, J.-H. Im, K.-B. Lee, T. Moehl, A. Marchioro, S.-J. Moon, R. Humphry-Baker, J.-H. Yum, J.-E. Moser, M. Grätzel, N.-G. Park, Lead iodide perovskite sensitized all-solid-state submicron thin film mesoscopic solar cell with efficiency exceeding 9%, Scientific reports 2 (2012) 591. doi:10.1038/srep00591.

[4] J. ichi Fujisawa, T. Eda, M. Hanaya, Comparative study of conduction-band and valence-band edges of tio2, srtio3, and batio3 by ionization potential measurements, Chemical Physics Letters 685 (2017) 23–26. doi:https://doi.org/10.1016/j.cplett.2017.07.031.

[5] G. Zhang, Y. Bai, R. Li, D. Shi, S. Wenger, S. M. Zakeeruddin, M. Grätzel, P. Wang, Employ a bisthienothiophene linker to construct an organic chromophore for efficient and stable dye-sensitized solar cells, Energy Environ. Sci. 2 (2009) 92–95. doi:10.1039/B817990E.